Numerical investigation on retrieval errors of mixing states of fractal black carbon aerosols using single-particle soot photometer based on Mie scattering and the effects on radiative forcing estimation

Jia Liu[1, 2, 3], Guang-ya Wang[1, 2, 3], Can-can Zhu[1, 2, 3], Dong-hui Zhou[1, 2, 3], and Lin Wang[1, 2, 3]

[1]Non-destructive Testing Laboratory, School of Quality and Technical Supervision, Hebei University, Baoding, 071002, China.
[2]National & Local Joint Engineering Research Center of Metrology Instrument and System, Baoding, 071002, China.
[3]Hebei Key Laboratory of Energy Metering and Safety Testing Technology, Baoding, 071002, China.

Correspondence to: Jia Liu (liujia@hbu.edu.cn)

Abstract. The mixing state of black carbon (BC) aerosols, that is the diameter ratio of coated particle to BC core (D_p/D_c), can be retrieved by the single-particle soot photometer (SP2). However, the retrieved D_p/D_c contains errors, because the core-shell model and Mie scattering calculation are normally employed in the retrieval principle of SP2 and the spherical core-shell structure seriously deviated from the real morphology of coated BC. In this study, fractal models are constructed to represent thinly and thickly coated BC particles for optical simulations, the differential scattering cross-sections are selected as references to conduct optical retrieval of particle diameter (D_p) based on Mie theory, just like the retrieval principle of SP2, and the volume equivalent diameter of BC core (D_c) is the same for fractal and spherical models. Then, the retrieval errors of the mixing state (D_p/D_c) of BC are investigated from numerical aspects, and the estimation accuracy of BC radiative forcing is analyzed through the simple forcing efficiency (SFE) equation with SP2 retrieval results taken into consideration. Results show that SP2 retrieved D_p/D_c based on Mie theory underestimates the realistic D_p/D_c of coated BC at most particle sizes. The retrieval errors of D_p/D_c of thinly coated BC for both single-particle and particle groups are larger than these of thickly coated BC. In addition, evaluation errors of radiative forcing of coated BC caused by retrieval errors of SP2 are up to about 55% and 95% at 1064 and 532 nm, respectively. This study provides meaningful referential understandings of the retrieved D_p/D_c of SP2 based on Mie scattering.

1 Introduction

Black carbon (BC) produced from the incomplete combustion of biomass and fossil fuels is considered to be an important contributor to global warming (Zhang et al., 2021). Black carbon aerosols directly affect the climate by absorbing shortwave solar radiation to heat the atmosphere, and also indirectly affect the climate through the complex interaction with clouds (Zhao et al., 2022). The bare BC just emitted from the source has poor hygroscopicity, making it difficult to form cloud condensation nuclei (CCN) (Zhuang et al., 2013). When the hydrophobic BC is mixed with hydrophilic aerosol during the aging process, the mixed BC aerosol also becomes hydrophilic, which further acts as CCN and participates in microphysical processes of

clouds, thus affecting the effective radius and number density of cloud droplets, cloud volume and lifetime, and ultimately the climate (Ching et al., 2016). When deposited to the surface of snow and ice, BC further reduces the snow albedo and accelerates the melting process (Jacobson, 2004). In addition, BC aerosols also affect the air pollution process by altering the thermal structure of the planetary boundary layer, which further suppresses the vertical diffusion of air pollutants, enhances haze events, harms human health, and reduces atmospheric visibility (Huang et al., 2018).

The non-spherical fractal morphology of BC has attracted extensive attention. Freshly emitted black carbon particles are chain-like aggregates consisting of a large number of near-spherical monomers. During the aging process in the atmospheric environment, BC will be coated by other species, and their aggregate morphology tends to be more compact (China et al., 2013). Combined observation and simulation carried out by China et al. (2015) showed that Mie calculations provide reasonable approximations for compact soot above remote marine clouds, and the distinction of radiative forcing estimated using Mie theory and using discrete dipole approximation is within 12% for a high surface albedo. The aging process causes variations in the mixing states of BC particles and results in significant changes in the optical parameters including absorption properties, which in turn affects the radiative forcing of BC and brings great uncertainties to the assessment of the climate effects of BC (Wu et al., 2018; Zeng et al., 2019). Therefore, the measurement and monitoring of the mixing states of BC particles have drawn much attention in the field of atmospheric aerosol observation. Currently, the mixing states of rBC-containing particles are mainly characterized using the following methods: the particle diameter ratio of the whole particles to the BC core (D_p/D_c), the coating thickness (CT), the SP2 measured numerical fractions of thinly and thickly coated rBC, and the mass ratio of the coating material to the BC core (M_R). Single-particle soot photometer (SP2) can effectively retrieve the mixing state (D_p/D_c) of BC aerosol based on Mie scattering and has been widely used in field and laboratory observations. Liu et al. (2014) employed SP2 to measure the particle size and mixing state of BC aerosols in London during wintertime and analyzed their emission sources, results showed that the D_p/D_c of BC particles emitted from three types of sources in the west, southeast, and east were 1.28, 1.45 and 1.69, respectively. Liu et al. (2022) measured M_R under different time backgrounds with the assistance of the tandem system of a Couette centrifugal particle mass analyzer (CPMA) and an SP2 and verified that the mixing state of BC was affected by both relative humidity (RH) and pollutant concentrations. Zhang et al. (2020) employed SP2 to characterize fresh BC particles emitted from four different emission sources and found that coatings are often already present in freshly emitted BC particles, and diesel vehicles emit BC particles with the least coatings (D_p/D_c~1.25), while crop residues emit BC particles with the most coatings (D_p/D_c~1.75). The application of SP2 has remarkably improved the understanding of the mixing state of freshly emitted and aged BC particles.

The SP2 measures the mass and differential scattering cross-section of each single BC particle based on the combination of laser-induced incandescent light technology and light scattering measurement technology. In the optical cavity, when a coated BC particle vertically passes through the high-energy laser beam at a wavelength of 1064 nm, there are two scattering signal detectors collect the scattering signal over certain solid angles at forward and backward directions, respectively (Schwarz et al., 2006). Gao et al. (2007) developed the leading-edge-only (LEO) fit method to deal with the collected scattering signal for SP2 with position-sensitive detector, the undisturbed leading edge of the scattering signal was employed to construct a

Gaussian scattering function, then the Gaussian function can be used to determine the differential scattering cross-section of the BC-containing particle. On the other hand, for SP2 without position-sensitive detector, Moteki and Kondo (2008) proposed to measure the time-dependent differential scattering cross-section ($\Delta C_{sca}(t)$) as each particle flowing across the Gaussian laser beam, and the differential scattering cross-section for coated BC particles can be further obtained. In general, the coated particles rapidly absorb the laser energy, the coating is heated to vaporization at first, and then the refractory BC (rBC) is heated and emits incandescent light (Zhao et al., 2021). At 1064 nm wavelength, when the rBC with particle masses range between the lower and upper detection limits of SP2, the intensity of the incandescent light signal is proportional to the mass of rBC, and the volume equivalent particle diameter of rBC can be obtained based on the preset density (1.80g/cm^3) (Moteki and Kondo, 2010). Mie scattering theory, which assumes that coated BC particle has a concentric core-shell structure consisting of coating sphere and BC sphere, is usually employed to retrieve the optical equivalent diameter of the coated BC based on differential scattering cross-section measured by SP2 (Schwarz et al., 2008; Kompalli et al., 2021). Finally, the particle size ratio of the whole particle to the BC core (D_p/D_c) can be obtained. Experimental results obtained by Laborde et al. (2012) showed that Mie scattering theory can be employed to retrieve the coating thickness of aged BC particles based on SP2 measurements. However, comparisons conducted by Scarnato et al. (2013) revealed that the scattering and absorption of the internally mixed BC calculated by the discrete dipole approximation (DDA) and the Mie scattering theory may be considerably different at 1000 nm (close to the 1064 nm used by SP2). Moteki et al. (2014) emphasized that the optical properties simulated by Mie theory deviate from the SP2 observations as much as 40% affected by the total particle mass, the rBC mass, and the refractive index of oleic acid coating. Schwarz et al. (2015) also proposed that when the SP2 was used to quantify the water-uptake of BC particles coated by ammonium sulfate, the uncertainty of SP2 measured results was mainly caused by the significant deviations in predicting SP2 scattering properties of BC particles using Mie scattering. In summary, it can be deduced that there are unavoidable errors in the retrieved D_p/D_c based on Mie theory because the core-shell model used in the retrieval of optical equivalent particle size D_p does not conform to the non-spherical complex morphology of the coated BC particles. At present, the retrieval error in D_p/D_c of coated BC based on SP2 measurement results is difficult to be quantified directly through experimental investigations. Nevertheless, the rapid developments of both morphology modeling and optical simulation of coated BC particles provide an investigative strategy for evaluating the retrieval accuracy of D_p/D_c.

Based on the microscopic morphology of coated BC, a series of models have been constructed in previous studies to investigate the optical properties of BC. Wu et al. (2014) constructed a fractal closed-cell model with concentric bilayer spheres as monomers, the optical properties at 450~1000 nm were calculated using the multiple-sphere *T*-matrix method (MSTM) and found that the optical properties of the closed-cell model differ significantly from the calculated results of the core-shell model based on Mie scattering theory. Zeng et al. (2019) developed the coated-aggregate model, the calculated results using the MTSM show that extinction of coated BC is significantly enhanced due to the increase in scattering, and the enhancement depends on both the amount and hydrophilicity of the coatings. Kanngiesser and Kahnert (2018) designed a tunable model for the transition from film-coating to spherical-shell coating, optical calculations using the discrete dipole approximation (DDA) at 355 and 532 nm showed that the rapid and slow transitions of the coating have different effects on the scattering cross-

section, and the overlapping phenomenon (C_{ov}) between the BC monomers can also affect the scattering cross-section. In short, abundant models and numerical simulation algorithms of BC provide convenience for accurate calculation of BC optical properties and also create an effective way to quantify the possible errors of the mixing states D_p/D_c of BC retrieved by SP2. In addition, there have been a number of experimental studies demonstrating the importance of considering BC as fractional aggregates. He et al. (2015) developed three different fractal aggregate models to simulate three typical evolution stages of BC particles and demonstrated that the dynamic aging process and the fractal shape should be considered for accurate estimations of the radiation effects. Romshoo et al. (2022) calculated the optical properties of three fractal particle models, results showed that the aggregate representation performs well in modeling the light absorption coefficient, the single-scattering albedo, and the mass absorption cross-section for laboratory-generated BC particles with mobility diameters larger than 100 nm. The fractal aggregate model was selected by Forestieri et al. (2018) to model uncoated soot particles, optical calculation results were used to compare with experimentally measured optical properties at multiwavelength, they emphasized that the sphere model and Mie theory widely used in climate models may lead to obvious underprediction in absorption of BC. All these studies have demonstrated the excellent performances of fractal aggregates in the optical modeling of black carbon. However, the fractal particle models have not been employed in the SP2 retrieval research, and the retrieval errors of the soot D_p/D_c caused by morphological model selection also have not been evaluated.

In this study, numerical simulations are performed based on the observation wavelength and complex refractive index employed by SP2 from the perspective of quantifying the retrieval error of D_p/D_c. The typical fractal model of BC particles with preset volume fractions of BC core and coating are constructed according to field observations, and the optical simulation results are regarded as reference values of realistic particles. Then, the volume equivalent sphere of BC in the fractal model is employed as BC core of the core-shell model, and the optical equivalent particle diameter of the coated BC is retrieved based on the scattering properties of fractal model using Mie scattering theory, which is similar to the retrieval principle of SP2. The retrieved value of D_p/D_c of optically equivalent core-shell model can be obtained. Finally, comparative analyses of the differences between the retrieved D_p/D_c of the core-shell model and the preset $D_{p,v}/D_{c,v}$ of the fractal model enable the evaluation of the SP2 retrieval accuracy of BC particle mixing states from numerical aspects. Furthermore, the effect of retrieval errors of mixing states on the radiative forcing evaluation of BC is discussed using the simple forcing efficiency equation to provide insight into the possible errors when SP2 retrieval results are employed in climate modes.

2 Methodology

2.1 Model construction of BC aerosols

According to observations of electron microscope, the morphology of freshly emitted black carbon particles often appears as chain-like aggregates. The geometry of the bare BC can be constructed according to the well-known fractal aggregate framework, and the mathematical description is as follows (Sorensen, 2001):

$$N_s = k_f \left(\frac{R_g}{a_0} \right)^{D_f} , \quad (1)$$

$$R_g = \sqrt{\frac{1}{N} \sum_{i=1}^{N} r_i^2} , \quad (2)$$

where a_0 is the radius of monomers, N_s is the number of monomers, k_f is the fractal prefactor and D_f is the fractal dimension that control the morphology of BC aggregates. R_g is the radius of gyration which measures the spatial size of the aggregate, r_i is defined as the distance between the ith monomer and the mass center of the whole aggregate.

During the aging process in the atmosphere, the surface of BC will be covered by organic and inorganic salt, forming complex coating structures (Kholghy et al., 2013). In order to more accurately simulate BC particles, two fractal aggregate models that are suitable for the actual morphology of BC are selected for numerical simulation, as shown in **Figure 1(a, b)**, the closed-cell and coated-aggregate models stand for thinly coated BC and thickly coated BC, respectively. The mixing state is represented by the ratio of the volume equivalent sphere diameter of coated particle to that of BC core ($D_{p,v}/D_{c,v}$). In addition, as shown in **Figure 1(c)**, the core-shell model based on the spherical assumption and applicable for Mie scattering theory is constructed, and mixing state can be directly expressed by the ratio D_p/D_c. For the construction of closed-cell and coated-aggregate models, the tunable diffusion-limited aggregation (DLA) software developed by Wozniak et al. (2012) are used at first to generate bare BC fractal aggregate, then spherical coatings were added based on original aggregate (Liu et al., 2023). The ratio $D_{p,v}/D_{c,v}$ can be obtained from the volume fraction of BC core (V_f) according to the mathematical formula shown below:

$$V_f = \frac{V_{BC}}{V_{total}} , \quad (3)$$

$$\frac{D_{p,v}}{D_{c,v}} = \frac{1}{\sqrt[3]{V_f}} , \quad (4)$$

$$D_{c,v} = 2a_0 \sqrt[3]{N_s} , \quad (5)$$

where V_{BC} and V_{total} are the volume of BC core and the whole coated BC particle, respectively.

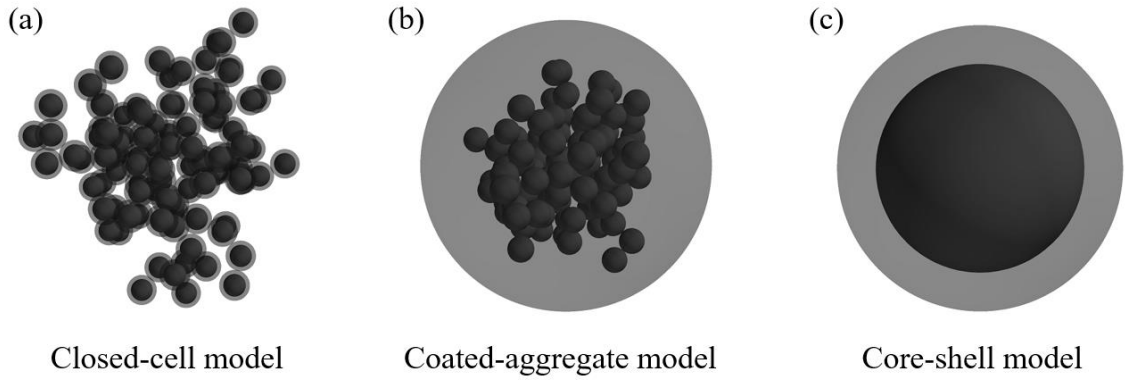

Figure 1. Geometries of fractal BC aggregate model with N_s=100 and core-shell model. **(a)** Closed-cell model with D_f =2.4 and V_f =0.40. **(b)** Coated-aggregate model with D_f =2.6 and V_f =0.10. **(c)** Core-shell model with V_f =0.40.

In this study, the value of fractal prefactor (k_f) is assumed to be 1.20 (Sorensen and Roberts, 1997), and the radius of BC monomer (a_0) is fixed at 20 nm which is a typical value observed in experiments (Li et al., 2003). Meanwhile, N_s ranges from 50 to 2000 with a step size of 50, which covers the D_c measured by SP2. The remaining microphysical parameters D_f and V_f also affect the morphology of the fractal aggregate model, and the corresponding relationships between $D_{p,v}/D_{c,v}$ and V_f are shown in **Table 1**.

Table 1. Morphological descriptors of BC fractal aggregate model.

	Parameters	Values
All	monomer radius (a_0)	20 (nm)
All	Monomer numbers (N_s)	50-2000, step length 50
All	Fractal prefactor (k_f)	1.20
Thinly coated	Fractal dimension (D_f)	1.80, 2.40, 2.60
	Volume fraction (V_f)	0.70, 0.40, 0.10, 0.075, 0.05
	Volume equivalent diameter ratio of shell/core ($D_{p,v}/D_{c,v}$)	1.13, 1.36, 2.15, 2.37, 2.71
Thickly coated	Fractal dimension (D_f)	2.60, 2.80
	Volume fraction (V_f)	0.10, 0.075, 0.05
	Volume equivalent diameter ratio of shell/core ($D_{p,v}/D_{c,v}$)	2.15, 2.37, 2.71

2.2 Numerical simulation of optical properties

Many methods have been used to calculate the optical properties of BC fractal aggregates, such as the Rayleigh-Debye-Gans (RDG) approximation, the discrete dipole approximation (DDA), and the *T*-matrix method (Adachi et al., 2010; Li et al., 2016; Mishchenko et al., 2013). As one of the most computationally efficient and accurate methods, the multiple-sphere *T*-matrix method (MSTM) is developed based on *T*-matrix theory and employs the addition theorem of vector spherical wave functions to account for the interactions between different spherical monomers in multi-sphere systems (Mackowski, 2014). The MSTM code has been widely used in numerical simulation studies to calculate the optical properties of BC fractal aggregates (He et

al., 2015). The wavelength of the optical property simulation is set to 1064 nm in this study, which is the same as the laser wavelength used in the SP2. Typically, the refractive indices of BC core and coating materials were assumed to be 2.26-1.26*i* and 1.50+0*i* respectively, and the densities of BC core (ρ_{BC}) and coatings ($\rho_{coating}$) were set to 1.80 g/cm^3 and 1.20 g/cm^3 (Zhang et al., 2019; Liu et al., 2014; Turpin and Lim, 2001). In addition, the selections of the refractive index and density are consistent for both MSTM calculation and Mie scattering calculation.

The two scattering signal detectors of the SP2 are distributed at forward scattering and backward scattering directions, which have view angles (θ) range in 13-77° and 103-167°, respectively (Wu et al., 2023). And the solid angle ($\Delta\Omega$) of light collection for the detectors can be calculated according to (Moteki and Kondo, 2007):

$$\Delta\Omega = \int_{\Delta\varphi} d\varphi \int_{\Delta\theta} \sin\theta d\theta \,, \tag{6}$$

where the azimuth angle (φ) ranges from 60° to 120°. Furthermore, the differential scattering cross-section of the coated soot particle is as follows:

$$\frac{dC_{sca}}{d\Omega} = \frac{F_{11}}{k^2} \,, \tag{7}$$

where F_{11} is the scattering phase function, k=2π/λ denotes the wavenumber.

2.3 Retrieval of mixing state of BC

The detected incandescent signals of SP2 can be employed to determine the mass of each single BC core, then the diameter of the BC core (D_c) can be deduced based on its density. The leading-edge-only (LEO) fit method developed by Gao et al. (2007) constructs a complete Gaussian scattering function using the scattering signal of each coated BC particle before it is perturbed by the laser, and the Gaussian scattering function can be used to determine the differential scattering cross-section of the coated BC particle. Further, the diameter of coated BC particles (D_p) can be retrieved using Mie scattering theory. Based on the retrieval principle of SP2, the retrieval of mixing state D_p/D_c with the differential scattering cross-section of fractal soot particle as a reference is the key of this study.

The specific retrieval process is shown in **Figure 2**. Firstly, the differential optical property of the BC fractal aggregate models with preset $D_{p,v}/D_{c,v}$ at 1064 nm are calculated based on MSTM code. Secondly, the optical properties of the core-shell model are calculated using Mie scattering theory, with the value of D_c is the same as the $D_{c,v}$. Lastly, the core-shell model whose differential scattering cross-section has the smallest difference from that of fractal aggregate model is retrieved, and its D_p/D_c is regarded as the retrieved mixing state of coated BC particle. Furthermore, a simplified conceptual retrieval method based on ordinary least squares was defined as follows:

$$\chi^2 = \left[\frac{dC_{sca-MSTM}\left(D_{p,v}\right) - dC_{sca-Mie}\left(D_p\right)}{dC_{sca-MSTM}\left(D_{p,v}\right)} \right]^2, \quad (8)$$

where $dC_{sca\text{-}MSTM}$ and $dC_{sca\text{-}Mie}$ are the simulated differential scattering cross-sections of BC fractal aggregate models and core-shell models, respectively. In addition, the relative error (*RE*) is used to represent the mixing state retrieval error of BC:

$$RE = \frac{D_p/D_c - D_{p,v}/D_{c,v}}{D_{p,v}/D_{c,v}} \times 100\%, \quad (9)$$

Figure 2 also shows the verification process when SP2 retrieval results are used to predict the optical properties of coated BC at 532 nm. The optical properties of BC fractal aggregate models with the preset particle size ($D_{p,v}$) and the core-shell model with the retrieved particle size (D_p) at 532 nm are calculated based on the MSTM code and Mie scattering theory, respectively. The calculated normalized scattering and absorption properties is shown in section 3.3.

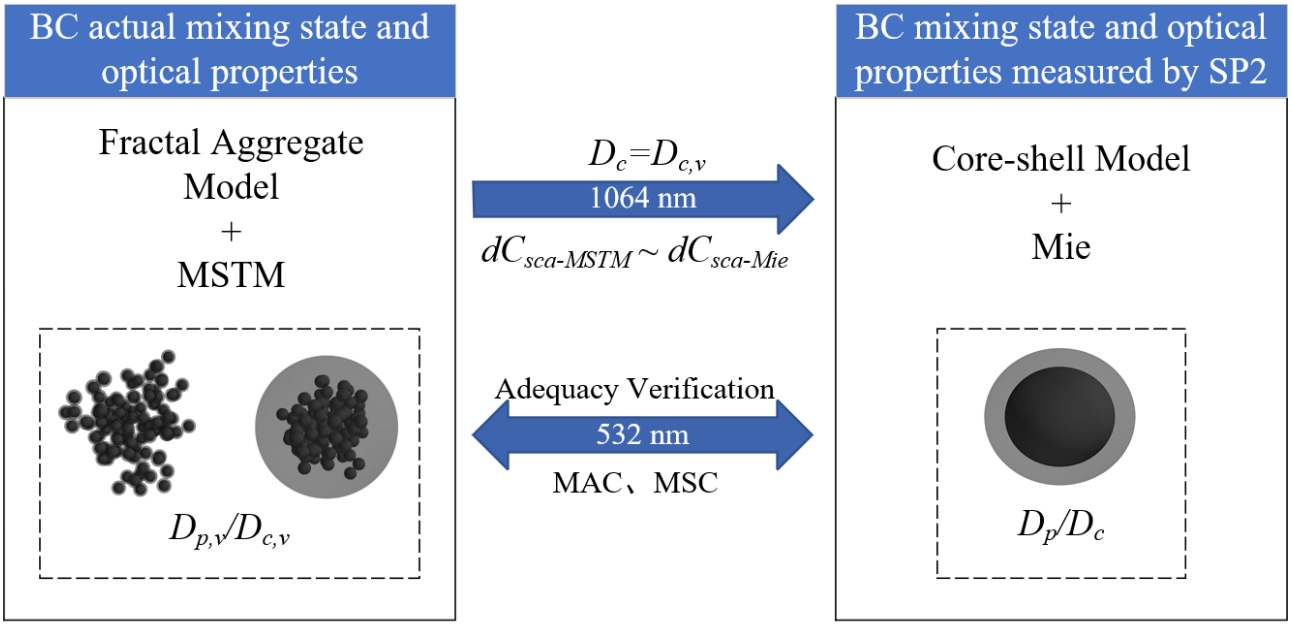

Figure 2. Schematic overview of the methodology of both the BC mixing state retrieval, and the verification of optical property at 532 nm predicted based on SP2 retrieval results.

3 Result and discussion

3.1 Effect of BC aerosol morphology on the retrieval of mixing state

Figure 3 shows the retrieval results and relative errors (*RE*) of mixing states of thinly coated soot under different fractal dimensions (D_f) and volume equivalent particle diameter ratio shell/core ($D_{p,v}/D_{c,v}$), the colored lines and bars stand for

retrieved D_p/D_c and *RE*, respectively. The black dashed line in each figure is the preset value of $D_{p,v}/D_{c,v}$. Since the shell is larger than the core for core-shell model, a lower limit (D_p/D_c =1) exists for the retrieval results. **Figure S1** shows the variation of differential scattering cross-sections with coated particle diameter D_p of core-shell models with different core diameter (D_c=252.0 nm, 337.4 nm, 447.5 nm), where the solid and dotted lines indicate differential scattering cross-sections integral from 13° to 77° and from 103° to 167°, respectively. There are maximum and minimum values of the forward and backward differential scattering cross-sections, respectively, and there are apparent differences in the corresponding optical properties of fractal models and core-shell models, so the value of D_p for some fractal soot particles cannot be retrieved, leading to missed points in the figures of retrieved results of D_p/D_c and *RE*. For the thinly coated soot with $D_{p,v}/D_{c,v}$ larger than 2.15, as shown in **Figure 3(a-c)**, most of the relative errors of retrieved D_p/D_c are negative, especially for soot aerosols with larger preset $D_{p,v}/D_{c,v}$ and fractal dimension, which indicates that SP2 underestimates D_p/D_c of these coated soot particles. The retrieval results of D_p/D_c at different fractal dimensions have similar variation trends with the increase of the volume equivalent diameter of soot core. The D_p/D_c of all the preset $D_{p,v}/D_{c,v}$ can be retrieved for the closed-cell model with D_f =1.8, however, fewer results can be retrieved as fractal dimension increases, thus the retrieved D_p/D_c of SP2 may lose data of large amounts of slightly aged and compact atmospheric BC. In addition, as the fractal dimension decreases, the retrieved results become smaller while the absolute values of the relative error become larger. It should be noted that some different phenomenon appears in the retrieved mixing state when the preset $D_{p,v}/D_{c,v}$ is small and the fractal dimension is large. As can be seen from **Figure 3(d)**, the variations of retrieval results for closed-cell models with D_f =2.40 and 2.60 is different from that of **Figure 3(a-c)**, D_p/D_c can be well retrieved at small $D_{c,v}$. In addition, **Figure S2** demonstrates the retrieval results for $D_{p,v}/D_{c,v}$ =1.13, similarly, the at small D_p/D_c cannot be retrieved for closed-cell models with D_f =2.40 and 2.60. **Figure 4** shows the retrieval results and relative errors (*RE*) of mixing states of thickly coated particles. It can be seen that although the retrieval results for thickly coated BC particles also have missed points, the overall trend is clear and consistent at different particle fractal dimensions, and the largest RE of coated particles is about -62%. With the increase of particle size, the retrieval results of D_p/D_c also gradually converge to 1. Overall, the relative error of D_p/D_c for thickly coated BC particles is smaller than that of thinly coated BC particles, and the retrieval results for thickly coated BC particles cover wider range of particle sizes, which suggests that SP2 is more accurate in measuring the mixing state of thickly coated BC particles than that of thinly coated BC particles.

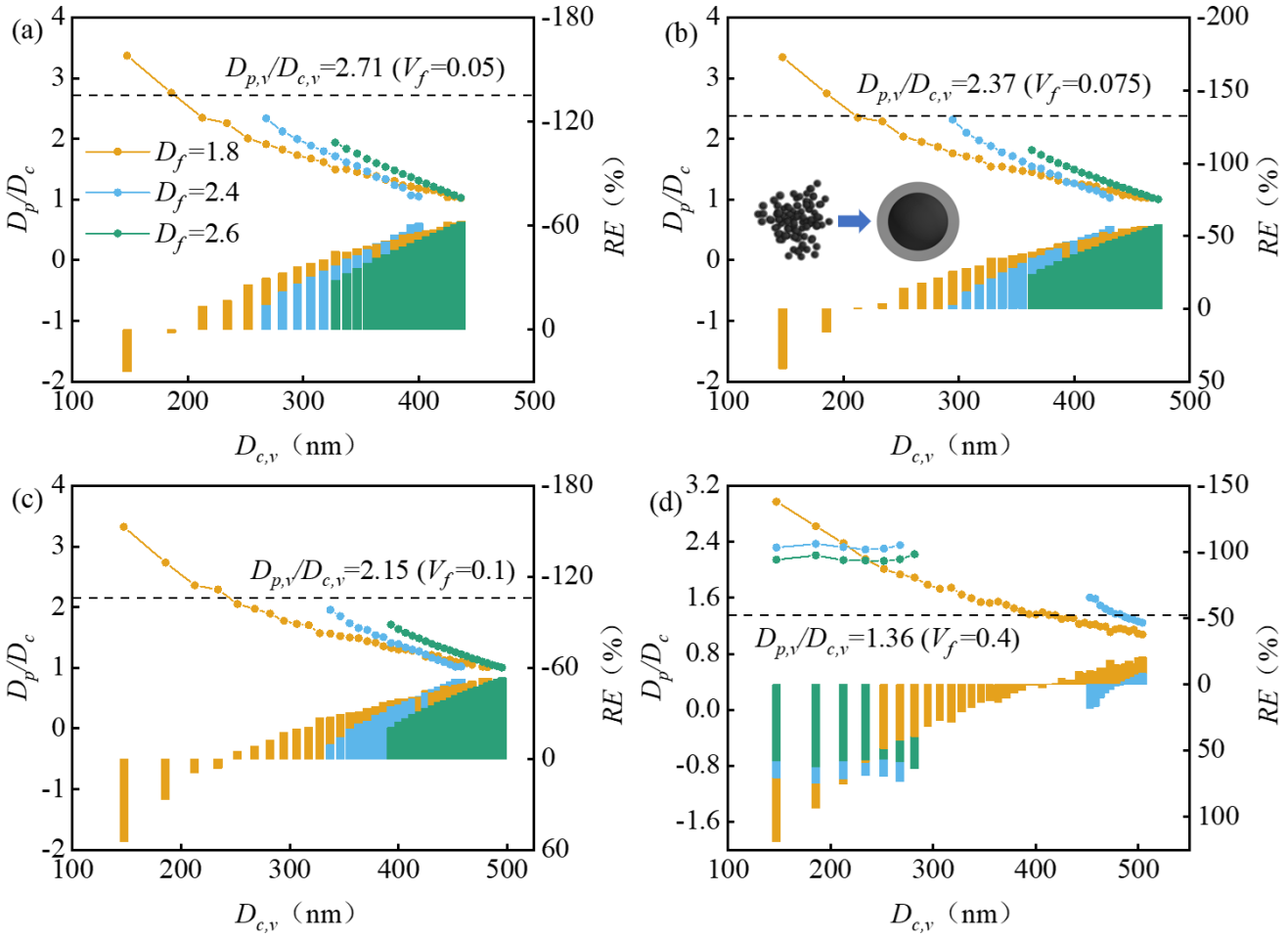

Figure 3. Retrieved mixing state (D_p/D_c) and relative error (*RE*) as functions of volume equivalent diameter ($D_{c,v}$) for thinly coated BC particles with different D_f and $D_{p,v}/D_{c,v}$. The colored lines stand for retrieved D_p/D_c and the colored bars stand for *RE*.

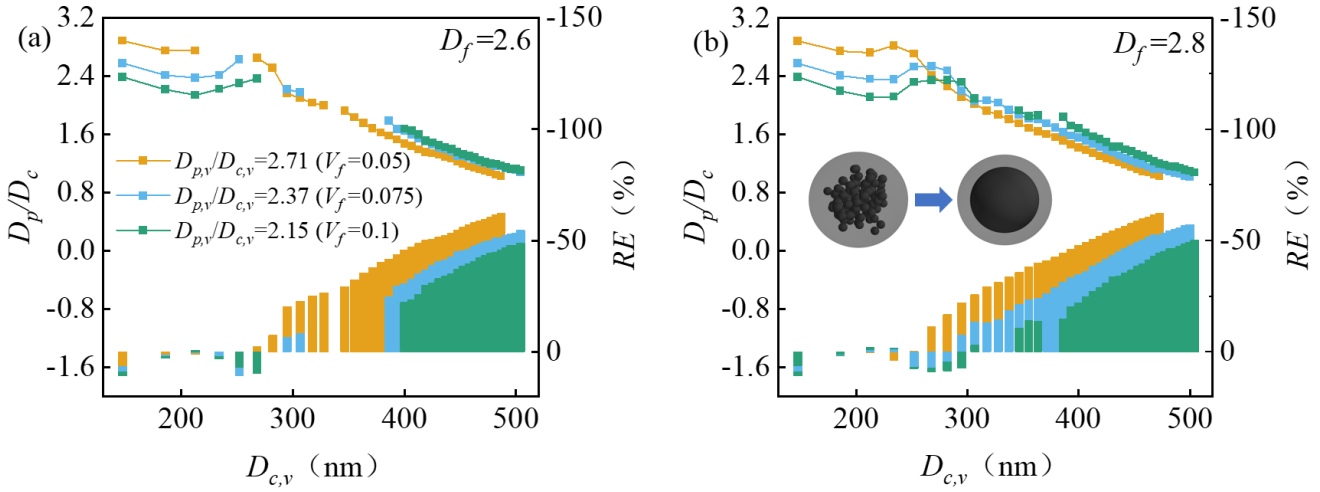

Figure 4. Retrieved mixing state (D_p/D_c) and relative error (*RE*) as functions of volume equivalent diameter ($D_{c,v}$) for thickly coated BC particles with different D_f and $D_{p,v}/D_{c,v}$. (a) Coated-aggregates with D_f = 2.60; (b) Coated-aggregates with D_f = 2.80. The colored lines stand for retrieved D_p/D_c and the colored bars stand for *RE*.

The distribution of retrieved results of mixing states for single-particle with different fractal dimensions over the entire particle size range is shown in **Figure 5**, and the filling width represents the probability distribution of retrieved D_p/D_c. As mentioned above, when $D_{p,v}/D_{c,v}$ decreases and D_f increases, D_p/D_c of some coated soot particles cannot be retrieved, that why the data point for $D_{p,v}/D_{c,v}$=1.13 and 1.36 is smaller than other three points, especially for $D_{p,v}/D_{c,v}$=1.13. Therefore, the particle mixing states with large amount of missed retrieval results are not considered in both the prediction adequacy verification of optical properties and the radiative forcing of aged soot aerosols in Sections 3.3 and 3.4. In general, the mean value of retrieved D_p/D_c decreases as the preset $D_{p,v}/D_{c,v}$ decreases. It can be seen from the figures that the probability distribution of retrieved mixing states are similar for particles employing the same model. The retrieved D_p/D_c for soot with more compact structures have higher retrieval accuracy, and the distributions are more uniform. As for the comparison of these two morphological models for soot with different aging state, the retrieved D_p/D_c of coated-aggregate model is closer to the preset values, which confirms that the mixing state retrieval error of SP2 is relatively smaller for thickly coated BC particles.

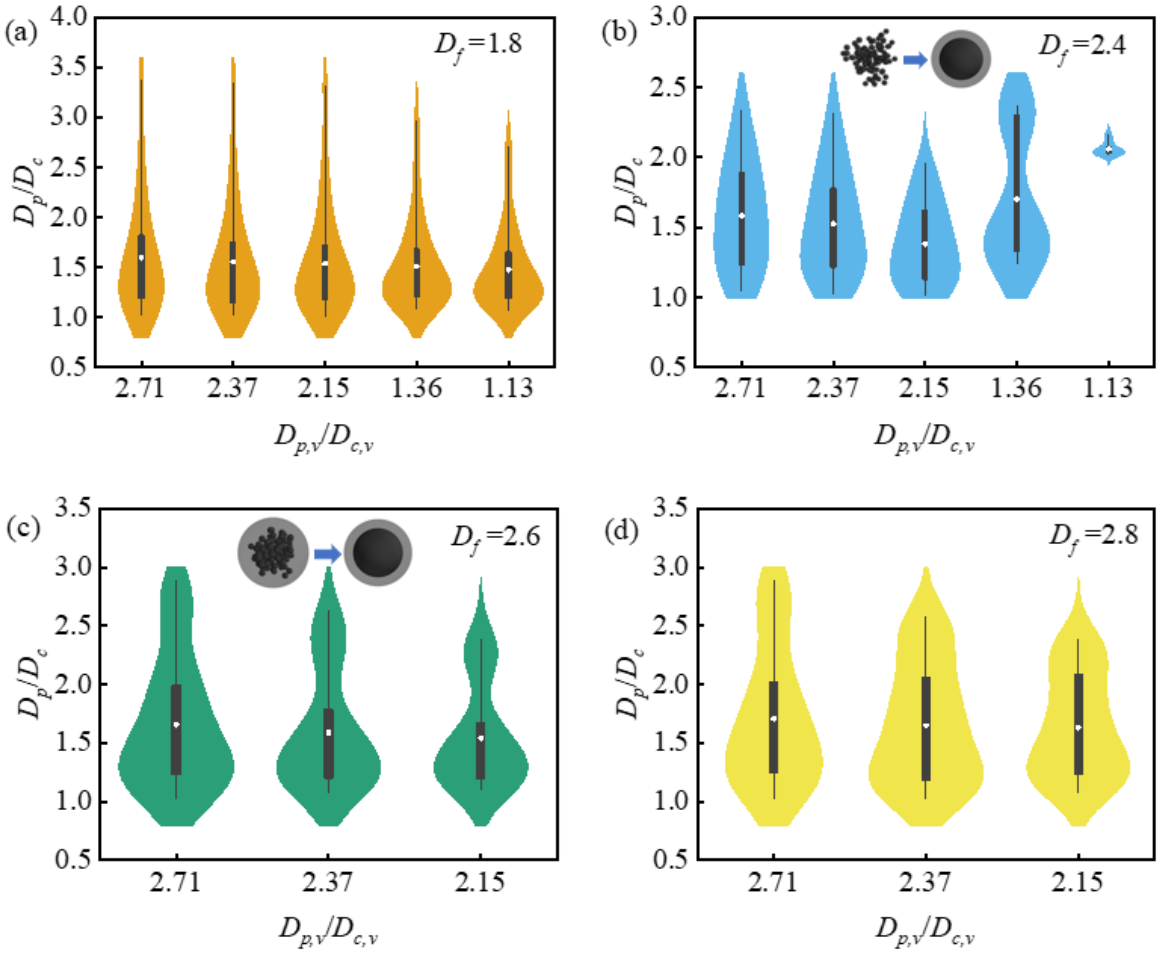

Figure 5. The distributions of retrieved D_p/D_c for different models with different fractal dimensions. (a) thinly coated BC with D_f =1.80; (b) thinly coated BC with D_f =2.40; (c) thickly coated BC with D_f =2.60; (d) thickly coated BC with D_f =2.80. The black box represents the 25th and the 75th percentiles, the whisker represents the maximum and minimum values of the retrieved results, and the white dot in box represents the average value of retrieved D_p/D_c.

3.2 Retrieved mixing state for particles with a certain size distribution

It is known from previous observations and experiments that the bulk optical properties of realistic atmospheric BC particles are integrated over a certain particle size distribution. In order to better understand the accuracy of SP2 on the D_p/D_c retrieval results of the bulk BC particles, the retrieved results for particle groups are also considered in this study. It is assumed that the equivalent volume diameters of coated BC particles follow the log-normal distribution:

$$n(d) = \frac{1}{\sqrt{2\pi} d \ln(\sigma_g)} \exp\left[-\left(\frac{\ln(d) - \ln(d_g)}{\sqrt{2}\ln(\sigma_g)} \right)^2 \right], \quad (10)$$

where σ_g is the geometric standard deviation and d_g is the geometric mean diameter. d is the diameter of the sphere with the same volume as that of the whole coated BC aggregates (i.e., volume equivalent sphere). Particle size distribution of coated BC aggregates with d_g=0.15 μm (Yu and Luo, 2009) and σ_g=1.59 (Zhang et al., 2012) is considered, and these BC particles have the same preset D_p/D_c. The retrieved D_p/D_c and relative errors of the BC particles with size distribution mentioned above are shown in **Table 2**. For the thinly coated BC particles with D_f =1.80, retrieval results decrease with the increase of preset $D_{p,v}/D_{c,v}$, but there is not obvious regularity due to the missed retrieval results of the closed-cell models with D_f =2.40 and 2.60. In addition, the relative errors for closed-cell particle groups are larger than that of coated-aggregate particle groups.

Table 2. Retrieved D_p/D_c and relative errors of BC particle groups

	closed-cell model					
	D_f =1.80		D_f =2.40		D_f =2.60	
preset $D_{p,v}/D_{c,v}$	retrieved D_p/D_c	*RE*	retrieved D_p/D_c	*RE*	retrieved D_p/D_c	*RE*
2.71	1.49	-45.2%	1.31	-51.8%	1.25	-54.0%
2.37	1.51	-36.5%	1.28	-45.9%	1.20	-49.5%
2.15	1.53	-29.0%	1.21	-43.8%	1.18	-45.2%
1.36	1.69	24.4%	2.22	63.6%	2.15	58.7%
1.13	1.70	51.1%	2.05	81.6%	1.89	68.2%

	coated-aggregate model			
	D_f =2.60		D_f =2.80	
preset $D_{p,v}/D_{c,v}$	retrieved D_p/D_c	*RE*	retrieved D_p/D_c	*RE*
2.71	1.68	-38.1%	1.66	-38.7%
2.37	1.94	-18.4%	1.78	-25.0%
2.15	1.98	-8.0%	1.95	-9.3%

3.3 Verification of adequacy when SP2 retrieval results are employed to predict optical properties of BC

The optical equivalent diameter D_p and mixing state (D_p/D_c) can be retrieved by SP2 based on Mie scattering. Then, all the optical properties of black carbon particles or even optical properties at other wavelengths can be predicted based on Mie scattering calculation of core-shell model. In this study, the prediction accuracy of optical properties at 532 nm are selected as typical example. The optical simulation results of the fractal particle models are used to represent the optical properties of the actual atmospheric BC particles, while the optical properties of the core-shell model represent the predicted optical properties of the BC particles inferred from the SP2 retrieval results.

The radiative forcing of BC aerosol is closely related to the absorption and scattering properties. In order to investigate the effect of retrieval errors of SP2 caused by morphological model selection on the estimation of BC radiation effect, optical

properties mass scattering cross-section (MSC) and mass absorption cross-section (MAC) are calculated for further investigation:

$$\mathrm{MAC} = \frac{C_{sca}}{m_{BC}}, \tag{11}$$

$$\mathrm{MSC} = \frac{C_{abs}}{m_{total}}, \tag{12}$$

$$m_{BC} = \rho_{BC} V_{BC}, \tag{13}$$

$$m_{total} = \rho_{BC} V_{BC} + \rho_{coating} V_{coating}, \tag{14}$$

$$V_{coating} = \left(1 - V_f\right) V_{BC} / V_f, \tag{15}$$

where m_{BC} and m_{total} are the masses of the BC core and the whole coated BC particle, and $V_{coating}$ is the volume of coating material. The values of density of both BC and coating are mentioned in Section 2.2.

Figure 6 and **Figure 7** demonstrate the mass absorption cross-section and mass scattering cross-section of fractal models and core-shell models, respectively. The mass absorption cross-section of the closed-cell model slightly increases with the increase of both $D_{p,v}/D_{c,v}$ and D_f, but the size of BC core has little influence. The calculation results of the optical equivalent core-shell model based on SP2 retrieval results decrease with the increase of BC core size, and decrease with the increase of $D_{p,v}/D_{c,v}$ for large particles. Furthermore, the predicted MAC of coated particles is smaller than the actual MAC when the size of the BC core larger than about 260 nm. As shown in **Figure 6(c-d)**, the fractal dimension and mixing state have small effects on the mass absorption cross-section of the coated-aggregate model, but the differences in MAC between the coated-aggregate model and the core-shell model is apparent. This indicates that the predicted results of mass absorption cross-section deviate significantly from the actual values of the thickly coated BC particles, and the maximum relative error is up to about 78%.

Figure 7 demonstrates that the mass scattering cross-sections of the closed-cell model increases with particle size, fractal dimension and mixing state, and they are obviously larger than the corresponding results of the core-shell model in most cases over the entire particle size range, indicating that the predicted results of MSC based on SP2 retrieval results underestimate the mass scattering cross section of coated BC at 532 nm wavelength. In contrast, the mass scattering cross-sections of both the coated-aggregate model and the core-shell model decrease with the increase of particle size, as shown in **Figure 7(c-d)**, but the prediction error of the MSC is less of regularity and hard to parameterize.

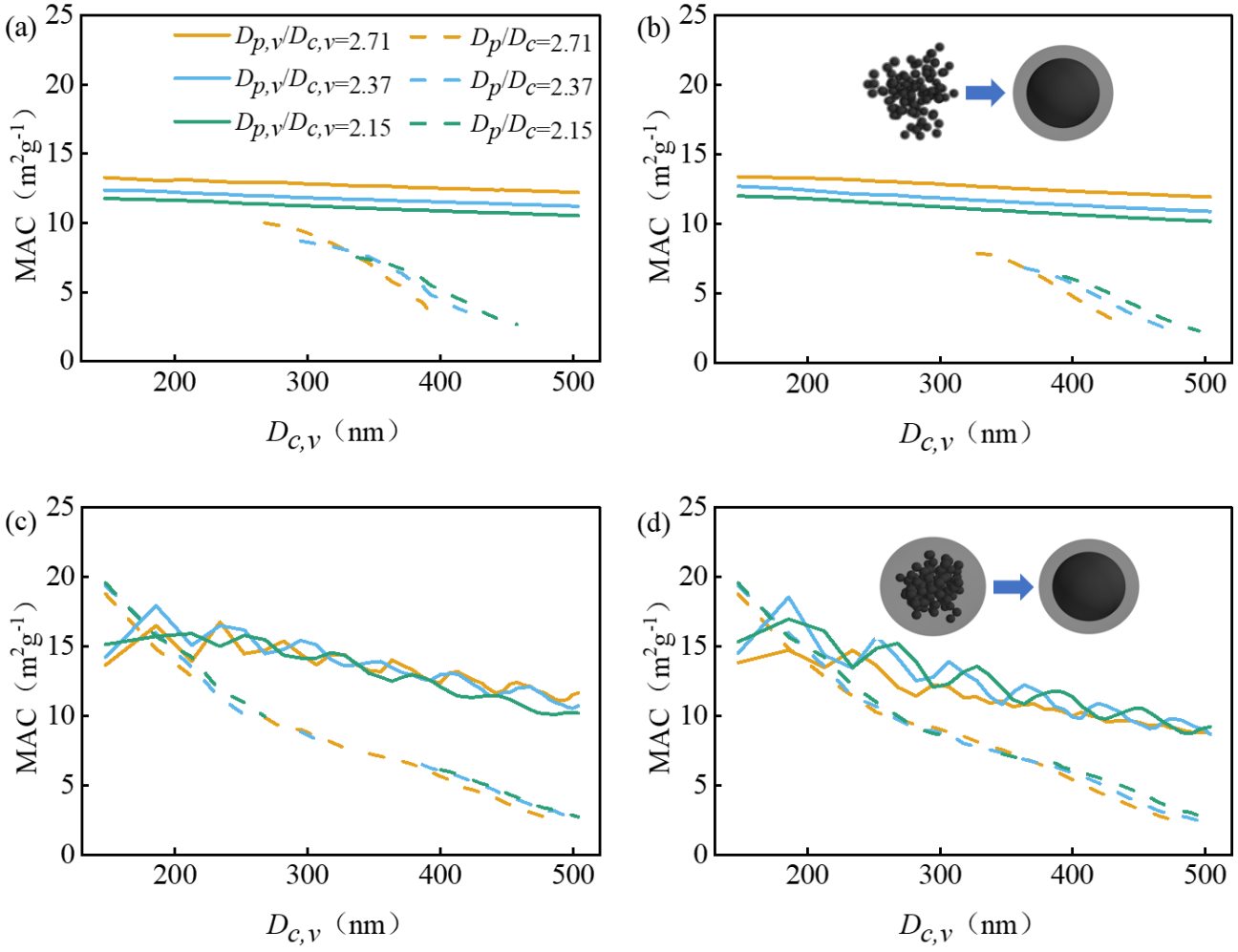

305 **Figure 6**. Differences in mass absorption cross-section (MAC) between fractal particle model (solid lines) and core-shell model (dashed lines) at 532 nm. **(a)** Closed-cell model with D_f =2.40; **(b)** Closed-cell model with D_f =2.60; **(c)** Coated-aggregate model with D_f =2.60; **(d)** Coated-aggregate model with D_f =2.80.

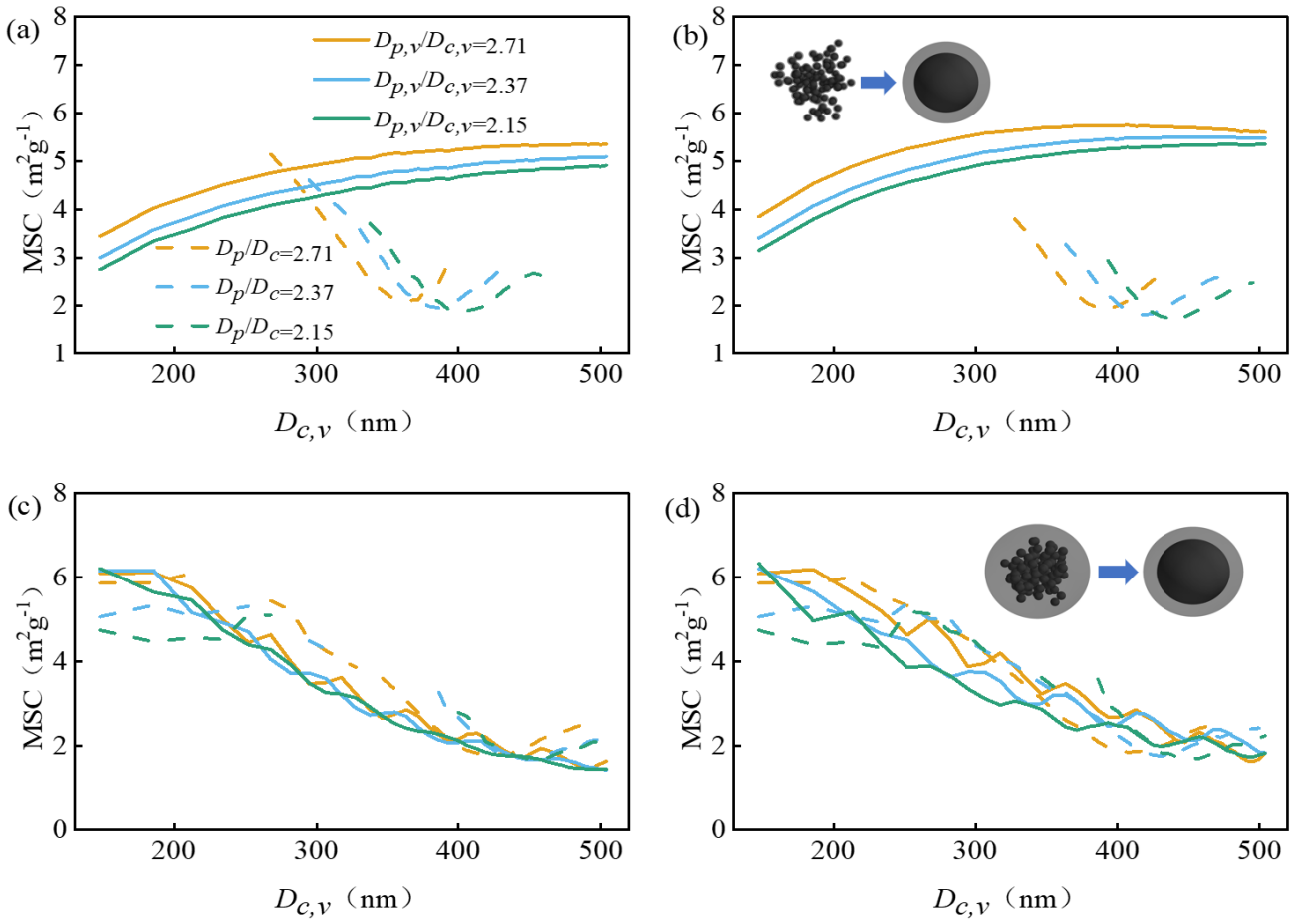

Figure 7. Similar to **Figure 6**, but the solid and dashed lines represent the mass scattering cross-section (MSC) of fractal particle model and core-shell model, respectively.

3.4 Effects of SP2 retrieval errors on the estimation of BC radiative forcing

The microphysical properties of black carbon (morphological structure, size distribution, and mixing state) have significant impacts on their optical properties, which further affect the radiative effect of black carbon. Lu et al. (2020) revealed that the uncertainty of the radiative forcing and heating rate of BC due to different geometries and size distributions of BC is less than 30%, while the uncertainty due to the mixing state of BC is as high as 80%. The SP2 retrieves the mixing state of BC based on the Mie scattering theory and BC particles are assumed to have spherical core-shell structures. But the core-shell model is seriously out of line with the actual morphology of BC, so the retrieved mixing state have unavoidable errors, which in turn affect the estimation of the radiative effect of BC. In this study, the simple forcing efficiency (SFE) equation developed by Bond and Bergstrom (2006) is employed to quantify the radiative forcing evaluation errors caused by mixing state retrieval errors of SP2. The SFE is defined as radiative forcing normalized by BC mass and represents the energy added to the Earth's atmospheric system by a given mass of particles in the atmosphere:

$$\frac{d\mathrm{SFE}}{d\lambda} = -\frac{1}{4}\frac{dS(\lambda)}{d\lambda}\tau^2\left(1-F_c\right)\left[2\left(1-a_s\right)^2\beta(\lambda)\times\mathrm{MSC}(\lambda)-4a_s\mathrm{MAC}(\lambda)\right], \quad (16)$$

where $\frac{dS(\lambda)}{d\lambda}$ is the spectral solar irradiance according to ASTM G173-03, the atmospheric transmittance τ=0.79, the cloud fraction F_c=0.6, typical urban surface albedo a_s=0.19, and the backscatter fraction β=0.15.

Table 3 and **Table 4** show the calculated results of SFE at 532 nm and 1064 nm, and it can be found that all the values of radiative forcing of coated BC particles are positive. The "actual value" is the SFE of actual thinly and thickly coated BC particles represented by closed-cell model and coated-aggregate model, the optical properties are obtained using MSTM. The "retrieved value" is the SFE obtained using recalculated MSC and MAC based on the optical equivalent core-shell models from SP2 retrieval results. The effects of SP2 retrieval error on SFE are disparate at different wavelengths, the relative errors for all the considered particles in this study range from -55.4% to 0.2% at 1064 nm and range from -94.5% to -69.2% at 532 nm. The distinctions of SFE between the closed-cell model and the corresponding optical equivalent core-shell model is larger than the distinctions of SFE between the coated-aggregate model and the core-shell model at 1064 nm, which indicates that the SP2 retrieval error has more significant influence on the radiative forcing of the thinly coated BC. In summary, the effects of the SP2 retrieval errors on the estimation of the radiative forcing of coated BC is noteworthy and cannot be ignored.

Table 3. The SFE values of both the core-shell models used to interpret the SP2 measurements and the fractal soot models at 1064 nm.

$D_{p,v}/D_{c,v}$	SFE	closed-cell			coated-aggregate	
		D_f =1.80	D_f =2.40	D_f =2.60	D_f =2.60	D_f =2.80
2.71	actual value	0.15	0.15	0.16	0.19	0.20
	retrieved value	0.08	0.10	0.08	0.13	0.13
	relative error	-45.2%	-35.4%	-48.5%	-33.0%	-34.2%
2.37	actual value	0.15	0.15	0.15	0.18	0.19
	retrieved value	0.08	0.08	0.07	0.19	0.19
	relative error	-49.2%	-44.5%	-53.6%	4.6%	-1.4%
2.15	actual value	0.15	0.15	0.15	0.16	0.19
	retrieved value	0.07	0.08	0.07	0.20	0.19
	relative error	-51.8%	-48.7%	-55.4%	26.1%	0.2%

Table 4. The SFE values of both the core-shell models used to interpret the SP2 measurements and the fractal soot models at 1064 nm.

$D_{p,v}/D_{c,v}$	SFE	closed-cell			coated-aggregate	
		D_f =1.80	D_f =2.40	D_f =2.60	D_f =2.60	D_f =2.80
2.71	actual value	1.14	1.14	1.14	1.16	1.14
	retrieved value	0.07	0.09	0.07	0.16	0.16
	relative error	-93.7%	-92.3%	-93.8%	-86.4%	-85.8%
2.37	actual value	1.06	1.07	1.08	1.23	1.23
	retrieved value	0.06	0.07	0.06	0.33	0.34
	relative error	-93.9%	-93.2%	-94.5%	-73.0%	-72.6%
2.15	actual value	1.02	1.01	1.02	1.27	1.28
	retrieved value	0.06	0.07	0.13	0.39	0.36
	relative error	-94.2%	-93.5%	-86.8%	-69.2%	-72.3%

4 Conclusions

BC aerosols have strong light absorption capacity compared with other atmospheric aerosols, and they can disturb the regional and global radiation balance and produce positive radiative forcing by absorbing solar radiation, which eventually leads to global warming. The content and structure of coating significantly change the mixing state (D_p/D_c) of black carbon particles, and the lens effect caused by coating has important and complicated effects on the optical properties of black carbon, which brings great uncertainty to the radiative effect and ultimately affects the accurate assessment of the climate effect of black carbon aerosols.

Single-particle soot photometer (SP2) employs the spherical core-shell model to represent coated BC particles, but this inappropriate model introduces errors to the D_p/D_c retrieval results and is not conducive to accurately obtaining the mixing

state of coated fractal BC particles in the atmosphere. This study quantifies the SP2 retrieval error of the mixing state of coated BC particles using typical fractal morphological models of both thinly and thickly coated BC from the perspective of numerical simulations and evaluates the effect of retrieval error on the estimation of radiative forcing of BC aerosols. The main conclusions are summarized as follows:

1. The mixing state of most BC particles retrieved by SP2 based on Mie scattering is underestimated compared with the realistic D_p/D_c. Relative error in the retrieved mixing state of single BC particles under different coating conditions is significantly different. The relative error of thinly coated BC particle represented by the closed-cell model is larger than that of thickly coated BC particle represented by the coated-aggregate model. With the decrease of fractal dimension, the relative errors of the mixing state of thinly coated BC particles with loose structures increase.

2. For BC groups whose particle size follows a certain log-normal distribution, the SP2 retrieval results of D_p/D_c will be underestimated. The relative errors of D_p/D_c for closed-cell model are larger than that for coated-aggregate model, indicating that the SP2 retrieval accuracy of the mixing state of thickly coated BC particles is better than that of thinly coated BC particles.

3. When the D_p/D_c retrieved by SP2 are used to predict optical properties of coated BC, it can be found that the predicted mass absorption cross-section (MAC) and mass scattering cross-section (MSC) at 532 nm recalculated based on core-shell model have significant discrepancies with that of realistic thinly and thickly coated BC particles. The largest difference between the predicted MAC and the reference value is up to about 78%.

4. The retrieval errors of mixing state have larger effects on the estimation accuracy of radiative forcing for thinly coated BC particles than that for thickly coated BC particles at both 1064 and 532 nm wavelengths. Furthermore, the relative error of estimated radiative forcing of thinly coated BC particles reaches about 55% at 1064 nm, while it reaches about 95% at 532 nm. This study is a pilot work for the characterization of possible retrieval errors in mixing states of coated soot aerosols using SP2 and Mie theory. For future work, more morphological models that are suitable for modeling the microstructure of coated soot aerosols should be considered, and unified parameterization schemes of retrieval errors are much needed. Furthermore, comprehensive field or laboratory studies for the validation of the possible errors in mixing states are also future directions worth the effort.

Funding. Natural Science Foundation of Hebei Province (D2021201002); Science and Technology Project of Hebei Education Department (QN2021013); High-level Talents Research Start Project of Hebei University (521000981417).

Acknowledgments. We particularly thank Dr. Mishchenko M. I. and Dr. Mackowski D. W. for the MSTM code. We also appreciate the support of the supercomputing center of Hebei University.

Disclosures. The authors declare no conflicts of interest relevant to this study.

Data availability. Processed data for this study are available online (https://doi.org/10.13140/RG.2.2.29017.90729).

References

Adachi, K., Chung, S. H., and Buseck, P. R.: Shapes of soot aerosol particles and implications for their effects on climate, Journal of Geophysical Research-Atmospheres, 115, 9, 10.1029/2009jd012868, 2010.

Bond, T. C. and Bergstrom, R. W.: Light absorption by carbonaceous particles: An investigative review, Aerosol Science and Technology, 40, 27-67, 10.1080/02786820500421521, 2006.

China, S., Mazzoleni, C., Gorkowski, K., Aiken, A. C., and Dubey, M. K.: Morphology and mixing state of individual freshly emitted wildfire carbonaceous particles, Nat Commun, 4, 2122, 10.1038/ncomms3122, 2013.

China, S., Scarnato, B., Owen, R. C., Zhang, B., Ampadu, M. T., Kumar, S., Dzepina, K., Dziobak, M. P., Fialho, P., Perlinger, J. A., Hueber, J., Helmig, D., Mazzoleni, L. R., and Mazzoleni, C.: Morphology and mixing state of aged soot particles at a remote marine free troposphere site: Implications for optical properties, Geophysical Research Letters, 42, 1243-1250, 10.1002/2014gl062404, 2015.

Ching, J., Riemer, N., and West, M.: Black carbon mixing state impacts on cloud microphysical properties: Effects of aerosol plume and environmental conditions, Journal of Geophysical Research-Atmospheres, 121, 5990-6013, 10.1002/2016jd024851, 2016.

Forestieri, S. D., Helgestad, T. M., Lambe, A. T., Renbaum-Wolff, L., Lack, D. A., Massoli, P., Cross, E. S., Dubey, M. K., Mazzoleni, C., Olfert, J. S., Sedlacek, A. J., Freedman, A., Davidovits, P., Onasch, T. B., and Cappa, C. D.: Measurement and modeling of the multiwavelength optical properties of uncoated flame-generated soot, Atmospheric Chemistry and Physics, 18, 12141-12159, 10.5194/acp-18-12141-2018, 2018.

Gao, R. S., Schwarz, J. P., Kelly, K. K., Fahey, D. W., Watts, L. A., Thompson, T. L., Spackman, J. R., Slowik, J. G., Cross, E. S., Han, J. H., Davidovits, P., Onasch, T. B., and Worsnop, D. R.: A novel method for estimating light-scattering properties of soot aerosols using a modified single-particle soot photometer, Aerosol Science and Technology, 41, 125-135, 10.1080/02786820601118398, 2007.

He, C., Liou, K. N., Takano, Y., Zhang, R., Zamora, M. L., Yang, P., Li, Q., and Leung, L. R.: Variation of the radiative properties during black carbon aging: theoretical and experimental intercomparison, Atmospheric Chemistry and Physics, 15, 11967-11980, 10.5194/acp-15-11967-2015, 2015.

Huang, X., Wang, Z., and Ding, A.: Impact of Aerosol-PBL Interaction on Haze Pollution: Multiyear Observational Evidences in North China, Geophysical Research Letters, 45, 8596-8603, 10.1029/2018gl079239, 2018.

Jacobson, M. Z.: Climate response of fossil fuel and biofuel soot, accounting for soot's feedback to snow and sea ice albedo and emissivity, Journal of Geophysical Research: Atmospheres, 109, n/a-n/a, 10.1029/2004jd004945, 2004.

Kanngiesser, F. and Kahnert, M.: Calculation of optical properties of light-absorbing carbon with weakly absorbing coating: A model with tunable transition from film-coating to spherical-shell coating, Journal of Quantitative Spectroscopy & Radiative Transfer, 216, 17-36, 10.1016/j.jqsrt.2018.05.014, 2018.

Kholghy, M., Saffaripour, M., Yip, C., and Thomson, M. J.: The evolution of soot morphology in a laminar coflow diffusion flame of a surrogate for Jet A-1, Combust. Flame, 160, 2119-2130, 10.1016/j.combustflame.2013.04.008, 2013.

Kompalli, S. K., Babu, S. N. S., Moorthy, K. K., Satheesh, S. K., Gogoi, M. M., Nair, V. S., Jayachandran, V. N., Liu, D. T., Flynn, M. J., and Coe, H.: Mixing state of refractory black carbon aerosol in the South Asian outflow over the northern Indian Ocean during winter, Atmospheric Chemistry and Physics, 21, 9173-9199, 10.5194/acp-21-9173-2021, 2021.

Laborde, M., Schnaiter, M., Linke, C., Saathoff, H., Naumann, K. H., Mohler, O., Berlenz, S., Wagner, U., Taylor, J. W., Liu, D., Flynn, M., Allan, J. D., Coe, H., Heimerl, K., Dahlkotter, F., Weinzierl, B., Wollny, A. G., Zanatta, M., Cozic, J., Laj, P., Hitzenberger, R., Schwarz, J. P., and Gysel, M.: Single Particle Soot Photometer intercomparison at the AIDA chamber, Atmospheric Measurement Techniques, 5, 3077-3097, 10.5194/amt-5-3077-2012, 2012.

Li, J., Liu, C., Yin, Y., and Kumar, K. R.: Numerical investigation on the angstrom ngstrom exponent of black carbon aerosol, Journal of Geophysical Research-Atmospheres, 121, 3506-3518, 10.1002/2015jd024718, 2016.

Li, J., Posfai, M., Hobbs, P. V., and Buseck, P. R.: Individual aerosol particles from biomass burning in southern Africa: 2, Compositions and aging of inorganic particles, Journal of Geophysical Research-Atmospheres, 108, 12, 10.1029/2002jd002310, 2003.

Liu, D., Allan, J. D., Young, D. E., Coe, H., Beddows, D., Fleming, Z. L., Flynn, M. J., Gallagher, M. W., Harrison, R. M., Lee, J., Prevot, A. S. H., Taylor, J. W., Yin, J., Williams, P. I., and Zotter, P.: Size distribution, mixing state and source apportionment of black carbon aerosol in London during wintertime, Atmospheric Chemistry and Physics, 14, 10061-10084, 10.5194/acp-14-10061-2014, 2014.

Liu, H., Pan, X., Wang, D., Liu, X., Tian, Y., Yao, W., Lei, S., Zhang, Y., Li, J., Lei, L., Xie, C., Fu, P., Sun, Y., and Wang, Z.: Mixing characteristics of black carbon aerosols in a coastal city using the CPMA-SP2 system, Atmospheric Research, 265, 10.1016/j.atmosres.2021.105867, 2022.

Liu, J., Wang, L., Wang, G. Y., and Zhang, X. H.: Numerical investigation on the accuracy of size information of fractal soot aerosols retrieved by lidar: Optical property, morphology effect, and parameterization scheme, Journal of Quantitative Spectroscopy & Radiative Transfer, 295, 12, 10.1016/j.jqsrt.2022.108435, 2023.

Lu, Q., Liu, C., Zhao, D. L., Zeng, C., Li, J., Lu, C. S., Wang, J. D., and Zhu, B.: Atmospheric heating rate due to black carbon aerosols: Uncertainties and impact factors, Atmospheric Research, 240, 9, 10.1016/j.atmosres.2020.104891, 2020.

Mackowski, D. W.: A general superposition solution for electromagnetic scattering by multiple spherical domains of optically active media, Journal of Quantitative Spectroscopy & Radiative Transfer, 133, 264-270, 10.1016/j.jqsrt.2013.08.012, 2014.

Mishchenko, M. I., Liu, L., and Mackowski, D. W.: T-matrix modeling of linear depolarization by morphologically complex soot and soot-containing aerosols, Journal of Quantitative Spectroscopy & Radiative Transfer, 123, 135-144, 10.1016/j.jqsrt.2012.11.012, 2013.

Moteki, N. and Kondo, Y.: Effects of mixing state on black carbon measurements by laser-induced incandescence, Aerosol Science and Technology, 41, 398-417, 10.1080/02786820701199728, 2007.

Moteki, N. and Kondo, Y.: Method to measure time-dependent scattering cross sections of particles evaporating in a laser beam, J. Aerosol. Sci., 39, 348-364, 10.1016/j.jaerosci.2007.12.002, 2008.

Moteki, N. and Kondo, Y.: Dependence of Laser-Induced Incandescence on Physical Properties of Black Carbon Aerosols: Measurements and Theoretical Interpretation, Aerosol Science and Technology, 44, 663-675, 10.1080/02786826.2010.484450, 2010.

Moteki, N., Kondo, Y., and Adachi, K.: Identification by single-particle soot photometer of black carbon particles attached to other particles: Laboratory experiments and ground observations in Tokyo, Journal of Geophysical Research-Atmospheres, 119, 1031-1043, 10.1002/2013jd020655, 2014.

Romshoo, B., Pohlker, M., Wiedensohler, A., Pfeifer, S., Saturno, J., Nowak, A., Ciupek, K., Quincey, P., Vasilatou, K., Ess, M., Gini, M., Eleftheriadis, K., Robins, C., Gaie-Levrel, F., and Muller, T.: Importance of size representation and morphology in modelling opticalproperties of black carbon: comparison between laboratory measurements andmodel simulations, Atmospheric Measurement Techniques, 15, 6965-6989, 10.5194/amt-15-6965-2022, 2022.

Scarnato, B. V., Vahidinia, S., Richard, D. T., and Kirchstetter, T. W.: Effects of internal mixing and aggregate morphology on optical properties of black carbon using a discrete dipole approximation model, Atmospheric Chemistry and Physics, 13, 5089-5101, 10.5194/acp-13-5089-2013, 2013.

Schwarz, J. P., Perring, A. E., Markovic, M. Z., Gao, R. S., Ohata, S., Langridge, J., Law, D., McLaughlin, R., and Fahey, D. W.: Technique and theoretical approach for quantifying the hygroscopicity of black-carbon-containing aerosol using a single particle soot photometer, J. Aerosol. Sci., 81, 110-126, 10.1016/j.jaerosci.2014.11.009, 2015.

Schwarz, J. P., Spackman, J. R., Fahey, D. W., Gao, R. S., Lohmann, U., Stier, P., Watts, L. A., Thomson, D. S., Lack, D. A., Pfister, L., Mahoney, M. J., Baumgardner, D., Wilson, J. C., and Reeves, J. M.: Coatings and their enhancement of black carbon light absorption in the tropical atmosphere, Journal of Geophysical Research-Atmospheres, 113, 10, 10.1029/2007jd009042, 2008.

Schwarz, J. P., Gao, R. S., Fahey, D. W., Thomson, D. S., Watts, L. A., Wilson, J. C., Reeves, J. M., Darbeheshti, M., Baumgardner, D. G., Kok, G. L., Chung, S. H., Schulz, M., Hendricks, J., Lauer, A., Karcher, B., Slowik, J. G., Rosenlof, K. H., Thompson, T. L., Langford, A. O., Loewenstein, M., and Aikin, K. C.: Single-particle measurements of midlatitude black carbon and light-scattering aerosols from the boundary layer to the lower stratosphere, Journal of Geophysical Research-Atmospheres, 111, 15, 10.1029/2006jd007076, 2006.

Sorensen and Roberts: The Prefactor of Fractal Aggregates, Journal of colloid and interface science, 186, 447-452, 10.1006/jcis.1996.4664, 1997.

Sorensen, C. M.: Light Scattering by Fractal Aggregates: A Review, Aerosol Science and Technology, 35, 648-687, 10.1080/02786820117868, 2001.

Turpin, B. J. and Lim, H.-J.: Species Contributions to PM2.5 Mass Concentrations: Revisiting Common Assumptions for Estimating Organic Mass, Aerosol Science and Technology, 35, 602-610, 10.1080/02786820119445, 2001.

Wozniak, M., Onofri, F. R. A., Barbosa, S., Yon, J., and Mroczka, J.: Comparison of methods to derive morphological parameters of multi-fractal samples of particle aggregates from TEM images, J. Aerosol. Sci., 47, 12-26, 10.1016/j.jaerosci.2011.12.008, 2012.

Wu, Y., Cheng, T. H., Zheng, L. J., Zhang, Y. G., and Zhang, L. L.: Particle size amplification of black carbon by scattering measurement due to morphology diversity, Environmental Research Letters, 18, 10, 10.1088/1748-9326/acaede, 2023.

Wu, Y., Cheng, T. H., Gu, X. F., Zheng, L. J., Chen, H., and Xu, H.: The single scattering properties of soot aggregates with concentric core-shell spherical monomers, Journal of Quantitative Spectroscopy & Radiative Transfer, 135, 9-19, 10.1016/j.jqsrt.2013.11.009, 2014.

Wu, Y., Cheng, T. H., Liu, D. T., Allan, J. D., Zheng, L. J., and Chen, H.: Light Absorption Enhancement of Black Carbon Aerosol Constrained by Particle Morphology, Environmental Science & Technology, 52, 6912-6919, 10.1021/acs.est.8b00636, 2018.

Yu, F. and Luo, G.: Simulation of particle size distribution with a global aerosol model: contribution of nucleation to aerosol and CCN number concentrations, Atmospheric Chemistry and Physics, 9, 7691-7710, 10.5194/acp-9-7691-2009, 2009.

Zeng, C., Liu, C., Li, J. N., Zhu, B., Yin, Y., and Wang, Y.: Optical Properties and Radiative Forcing of Aged BC due to Hygroscopic Growth: Effects of the Aggregate Structure, Journal of Geophysical Research-Atmospheres, 124, 4620-4633, 10.1029/2018jd029809, 2019.

Zhang, K., O'Donnell, D., Kazil, J., Stier, P., Kinne, S., Lohmann, U., Ferrachat, S., Croft, B., Quaas, J., Wan, H., Rast, S., and Feichter, J.: The global aerosol-climate model ECHAM-HAM, version 2: sensitivity to improvements in process representations, Atmospheric Chemistry and Physics, 12, 8911-8949, 10.5194/acp-12-8911-2012, 2012.

Zhang, X., Mao, M., Chen, H., and Tang, S.: The single scattering albedo Angstrom exponent of black carbon with brown coatings, Journal of Quantitative Spectroscopy and Radiative Transfer, 259, 10.1016/j.jqsrt.2020.107429, 2021.

Zhang, Y. X., Zhang, Q., Yao, Z. L., and Li, H. Y.: Particle Size and Mixing State of Freshly Emitted Black Carbon from Different Combustion Sources in China, Environmental Science & Technology, 54, 7766-7774, 10.1021/acs.est.9b07373, 2020.

Zhang, Y. X., Li, M., Cheng, Y. F., Geng, G. N., Hong, C. P., Li, H. Y., Li, X., Tong, D., Wu, N. N., Zhang, X., Zheng, B., Zheng, Y. X., Bo, Y., Su, H., and Zhang, Q.: Modeling the aging process of black carbon during atmospheric transport using a new approach: a case study in Beijing, Atmospheric Chemistry and Physics, 19, 9663-9680, 10.5194/acp-19-9663-2019, 2019.

Zhao, G., Tan, T. Y., Zhu, Y. S., Hu, M., and Zhao, C. S.: Method to quantify black carbon aerosol light absorption enhancement with a mixing state index, Atmospheric Chemistry and Physics, 21, 18055-18063, 10.5194/acp-21-18055-2021, 2021.

Zhao, G., Tan, T. Y., Hu, S. Y., Du, Z. F., Shang, D. J., Wu, Z. J., Guo, S., Zheng, J., Zhu, W. F., Li, M. R., Zeng, L. M., and Hu, M.: Mixing state of black carbon at different atmospheres in north and southwest China, Atmospheric Chemistry and Physics, 22, 10861-10873, 10.5194/acp-22-10861-2022, 2022.

Zhuang, B., Liu, Q., Wang, T., Yin, C., Li, S., Xie, M., Jiang, F., and Mao, H.: Investigation on semi-direct and indirect climate effects of fossil fuel black carbon aerosol over China, Theoretical and Applied Climatology, 114, 651-672, 10.1007/s00704-013-0862-8, 2013.

515